1

Special Issues on Design Optimization of Wind Turbine Structures

Karam Maalawi
National Research Centre, Mechanical Engineering Department, Cairo
Egypt

1. Introduction

A wind turbine is a device that exploits the wind's kinetic energy by converting it into useful mechanical energy. It basically consists of rotating aerodynamical surfaces (blades) mounted on a hub/shaft assembly, which transmits the produced mechanical power to the selected energy utilizer (e.g. milling or grinding machine, pump, or generator). A control system is usually provided for adjusting blade angles and rotor position to face the wind properly. All units are supported by a stiff tower structure, which elevates the rotor above the earth's boundary layer. There are two common types: horizontal-axis and vertical-axis wind turbines. In the former, which dominate today's markets, the blades spin about an axis perpendicular to the tower at its top (see Fig.1), while in the latter they spin about the tower axis itself. In fact, wind turbines have been used for thousands of years to propel boats and ships and to provide rotary power to reduce the physical burdens of man. From the earliest

Fig. 1. Offshore horizontal-axis wind turbine

times of recorded history, there is evidence that the ancient Egyptians and Persians used wind turbines to pump water to irrigate their arid fields and to grind grains (Manwell et al., 2009). The technology was transferred to Europe and the idea was introduced to the rest of the world. Early wind turbines were primitive compared to today's machines, and suffered from poor reliability and high costs. Like most new technology, early wind turbines had to go through a process of "learning by doing", where shortcomings were discovered, components were redesigned, and new machines were installed in a continuing cycle. Today, Wind turbines are more powerful than early versions and employ sophisticated materials, electronics and aerodynamics (Spera, 2009). Costs have declined, making wind more competitive clean energy source with other power generation options. Designers apply optimization techniques for improving performance and operational efficiency of wind turbines, especially in early stages of product development. It is the main aim of this chapter to present some fundamental issues concerning design optimization of the main wind turbine structures. Practical realistic optimization models using different strategies for enhancing blade aerodynamics, structural dynamics, buckling stability and aeroelastic performance are presented and discussed. Design variables represent blade and tower geometry as well as cross-sectional parameters. The mathematical formulation is based on dimensionless quantities; therefore the analysis can be valid for different wind turbine rotor and/or tower sizes. Such normalization has led to a naturally scaled optimization models, which is favorable for most optimization techniques. The various approaches that are commonly utilized in design optimization are also presented with a brief discussion of some computer packages classified by their specific applications. Case studies include blade optimization in flapping and pitching motion, yawing dynamic optimization of combined rotor/tower structure, and power output maximization as a measure of improving aerodynamic efficiency. Optimization of the supporting tower structure against buckling as well as the use of the concept of material grading for enhancing the aeroelastic stability of composite blades have been also addressed. Several design charts that are useful for direct determination of the optimal values of the design variables are introduced. This helps achieving, in a practical manner, the intended design objectives under the imposed design constraints. The proposed mathematical models have succeeded in reaching the required optimum solutions, within reasonable computational time, showing significant improvements in the overall wind turbine performance as compared with reference or known baseline designs.

2. General aspects of wind turbine design optimization

Design optimization seeks the best values of a set of n design variables represented by the vector, $\underline{X}_{nx1}$, to achieve, within certain m constraints, $\underline{G}_{mx1}(\underline{X})$, its goal of optimality defined by a set of k objective functions, $\underline{F}_{kx1}(\underline{X})$, for specified environmental conditions. Mathematically, design optimization may be cast in the following standard form (Rao, 2009): Find the design variables $\underline{X}_{nx1}$ that minimize

$$F(\underline{X}) = \sum_{i=1}^{k} W_{fi} F_i(\underline{X}) \tag{1a}$$

subject to

$$G_j(\underline{X}) \le 0 \text{ , } j=1,2,\ldots\ldots I \tag{1b}$$

$$G_j(\underline{X}) = 0 \text{ , } j=I+1,I+2,\ldots m \tag{1c}$$

$$0 \leqslant W_{fi} \leqslant 1$$
$$\sum_{i=1}^{k} W_{fi} = 1 \tag{1d}$$

If it is required to maximize $F_i(\underline{X})$, one simply minimizes $-F_i(\underline{X})$ instead. The weighting factors W_{fi} measure the relative importance of the individual objectives with respect to the overall design goal. Fig. 2 shows the general scheme of an optimization approach to design.

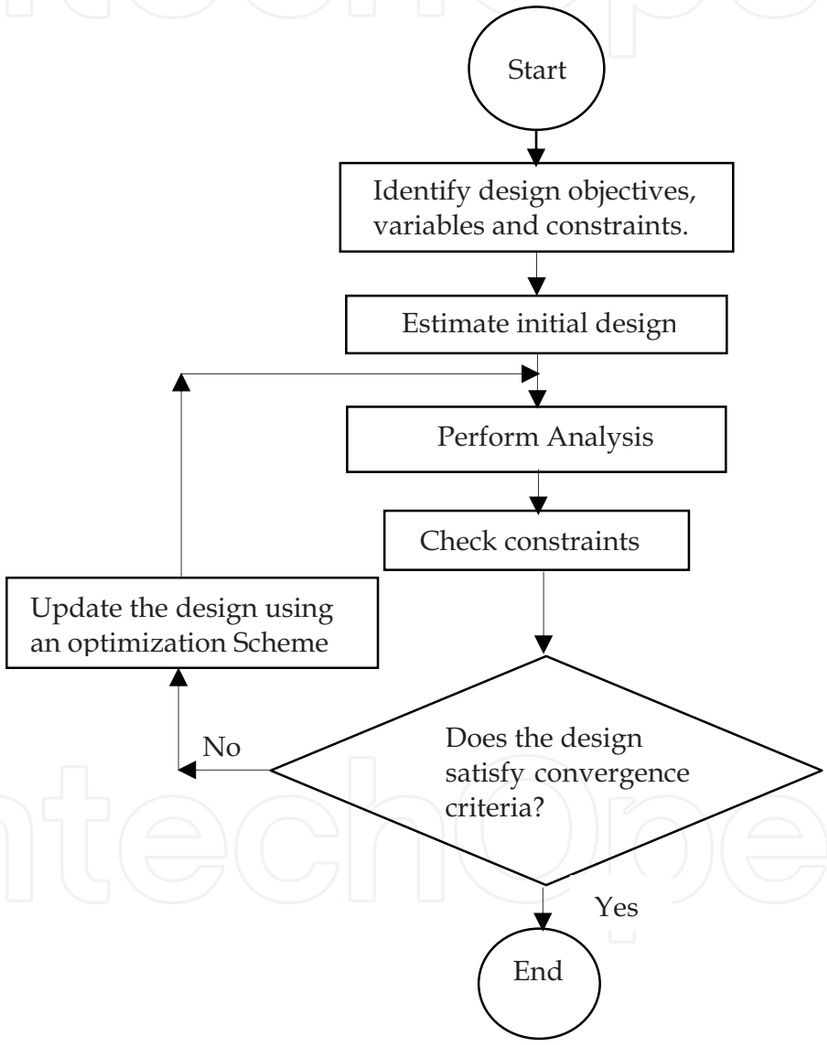

Fig. 2. Design optimization process

Several computer program packages are available now for solving a variety of design optimization models. Advanced procedures are carried out by using large-scale, general purpose, finite element-based multidisciplinary computer programs, such as *ASTROS* (Cobb et al., 1996), *MSC/NASTRAN* and *ANSYS* (Overgaard and Lund, 2005). The *MATLAB* optimization toolbox (Vekataraman, 2009) is also a poweful tool that includes many routines

for different types of optimization encompassing both unconstrained and constrained minimization algorithms. Design optimization of wind energy conversion systems involve many objectives, constraints and variables. This is because the structure of the wind turbine contains thousands of components ranging from small bolts to large, heavyweight blades and spars. Therefore, creation of a detailed optimization model incorporating, simultaneously, all the relevant design features is virtually imposible. Researchers and engineers rely on simplified models which provide a fairly accurate approximation of the real structure behaviour. In the subsequent sections, the underlying concepts of applying optimization theory to the design of a conventional wind turbine will be applied. The relevant design objectives, constraints and variables are identified and discussed.

2.1 Design objectives of a wind turbine

A successful wind turbine design should ensure efficient, safe and economic operation of the machine. It should provide easy access for maintenance, and easy transportation and erection of the various components and subcomponents. Good designs should incorporate aesthetic features of the overall machine shape. In fact, there are no simple criteria for measuring the above set of objectives. However, it should be recognized that the success of structural design ought to be judged by the extent to which the least possible cost of energy production can be achieved (Wei, 2010). For a specified site wind characteristics, the analysis of the unit energy cost (Euro/Kilowatt.Hour) involves many design considerations such as the rotor size, rated power, fatigue life, stability, noise and vibration levels.

2.2 Design variables

The definition of design variables and parameters is of great importance in formulating an optimization model. Design variables of a wind turbine include layout parameters as well as cross-sectional and spanwise variables. The main variables of the blades represent the type of airfoil section, chord and twist distributions, thickness of covering skin panels, and the spacing, size and shape of the transverse and longitudinal stiffeners. If the skin and/or stiffeners are made of layered composites, the orientation of the fibers and their proportion can become additional variables. Tower variables include type (truss- tubular), height, cross sectional dimensions, and material of construction.

2.3 Design constraints

There are many limitations that restrict wind turbine design, manufacturing and operation. The most significant among these are: (a) type of application (e.g. electricity generation), (b) site condition (location - wind speed characteristics - wind shear – transportation - local electricity system-…..), (c) project budget and financial limitations, (d) technological and manufacturing limitations, (e) manpower skills and design experience, (f) availability of certain material types, (g) safety and performance requirements. An optimal design for a wind turbine must achieve the system objectives and take into consideration all aspects of the design environments and constraints.

3. Basic aerodynamic optimization

The aerodynamic design of a wind turbine rotor includes the choice of the number of blades, determination of blade length, type of airfoil section, blade chord and twist distributions

and the design tip-speed ratio (TSR=rotational speed x rotor radius/design wind speed at hub height). Concerning blade number (N_B), a rotor with one blade can be cheaper and easier to erect but it is not popular and too noisy. The two-bladed rotor is also simpler to assemble and erect but produces less power than that developed by the three-bladed one. The latter produces smoother power output with balanced gyroscopic loads, and is more aesthetic. The determination of the blade length (or rotor size) depends mainly on the needed energy for certain application and average wind speed of a specific site. The choice of the type of airfoil section may be regarded as a key point in designing an efficient wind rotor (Burger & Hartfield 2006). Other factors that can have significant effects on the overall rotor design encompass the distribution of wind velocity in the earth boundary layer as well as in the tower shadow region (see Fig. 3).

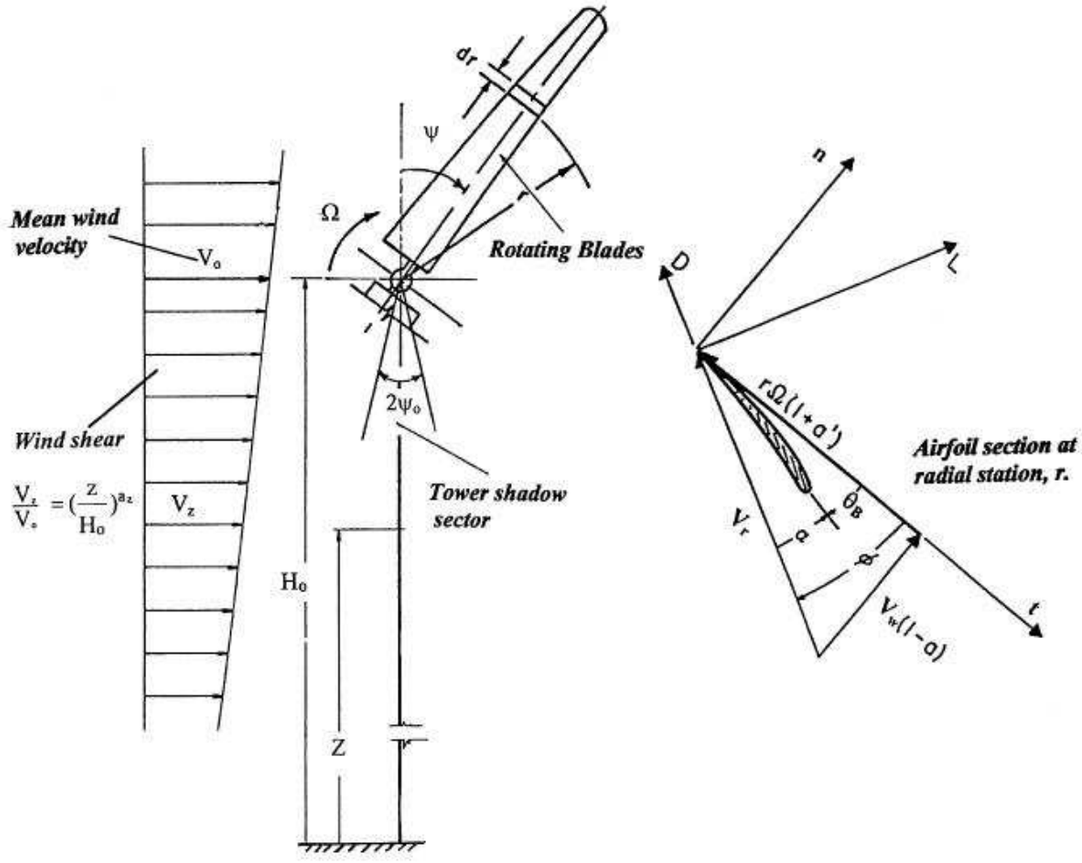

Fig. 3. Wind rotor geometry and velocity components

The various symobles in Fig. 3 are defined as follows: a=axial induction factor, a'=angular induction factor, a_z=wind shear exponent, D=aerodynamic drag, H_0=hub height, L=aerodynamic lift, r=local blade radius, V_r=resultant wind velocity, Z=height above ground or sea level, α=angle of attack, θ_B=blade twist, φ=inflow angle, ψ=azimuth angle, Ω=rotor rpm. More definitions can be found in (Maalawi & Badr, 2003). The following formula is used to calculate the output rated power P_r, or generator capacity of a wind turbine:

$$P_r = (C_p \eta) \frac{1}{2} \rho_{air} (\pi R^2) V_r^3 \text{ (Watts)} \quad (2)$$

Where:
C_p=power coefficient, depending on blade geometry , airfoil section and tip-speed ratio.
η = Transmission and generator efficiency.
R = Rotor radius (meter).
V_r =rated wind speed (m/s).
ρ_{air}= air density (kg/m^3).
An optimized wind rotor is that operates at its maximum power coefficient at the design wind speed, at which the design tip-speed ratio is set. This defines the rotor rpm and thus required gear ratio to maximize the energy production. The calculations of the annual energy productivity are accomplished by an iterative computer calculation based on the Weibul wind representation and the specified power performance curve (Wei, 2010). Operating the wind turbine at the design TSR corresponding to the maximum power point at all times may generate 20–30% more electricity per year. This requires, however, a control scheme to operate with variable speed. Several authors (Kusiak, et al, 2009), (Burger & Hartfield 2006), (Maalawi & Badr, 2003) have studied optimum blade shapes for maximizing C_p. Important conclusions drawn from such studies have shown that the higher the lift/drag ratio, the better the aerodynamic performance of the turbine. Analytical studies by (Maalawi & Badawy, 2001) and (Maalawi & Badr, 2003) indicated that the theoretical optimum distributions of the blade chord and twist can be adequately determined from an exact analysis based on Glauert's optimum conditions. The developed approach eliminated much of the numerical efforts as required by iterative procedures, and a unique relation in the angle of attack was derived, ensuring convergence of the attained optimal solutions. Based on such analytical approach, the theoretical optimum chord distribution of the rotating blade can be determined from the following expression:

$$C(r) = \frac{8\pi r F \sin\varphi}{N_B C_L \{[(\lambda_r + \tan\varphi)/(1 - \lambda_r \tan\varphi)] - (C_D / C_L)\}} \quad (3)$$

where N_B is the number of blades, C_D/C_L the minimum drag-to-lift ratio of the airfoil section, F tip loss factor, λ_r (=$\Omega r/V_o$) local speed ratio at radial distance *r* along the blade, Ω rotational speed of the blade and V_o wind velocity at hub height (refer to Fig. 3). Having determined the best blade taper and twist, the aerodynamic power coefficient can be calculated by integrating all of the contributions from the individual blade elements, taking into account the effect of the wind shear and tower shadow. Fig. 4 shows variation of the optimum power coefficient with the design tip-speed ratio for a blade made of NACA 4-digit airfoil families. Both cases with (lower curves) and without (upper curves)wind shear and tower shadows were investigated. It is seen that Cp increases rapidly with TSR up to its optimum value after which it decreases gradually with a slower rate. The optimum range of the TSR is observed to lie between 6 and 11, depending on the type of airfoil. The effect of wind shear and tower shadow resulted in a reduction of the power coefficient by about 16%. The value of the design TSR at which $C_{p,max}$ occurs is also reduced by about 9%. It is also observed that blades with NACA 1412 and 4412 produce higher power output as compared with other airfoil types.

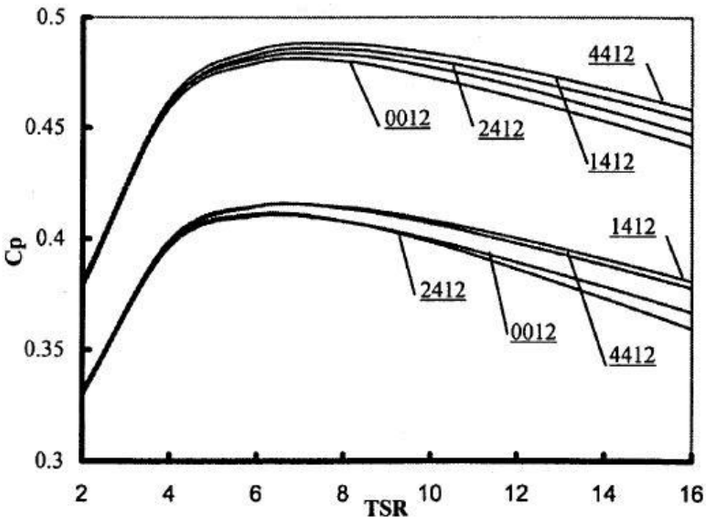

Fig. 4. Variation of the optimum power coefficent with tip-speed ratio for a three-bladed rotor made of NACA-4 digit airfoils

4. Frequency optimization models

Large horizontal-axis wind turbines (HAWT) utilized for electricity generation are characterized by their slender rotating blades mounted on flexible tall towers. Such a configuration gives rise to significant vibration problems, and assesses the importance of analyzing blade and tower dynamics in the design of successful wind generators. A major issue for reducing vibration levels is to avoid the occurrence of resonance, which plays a central role in the design of an efficient wind turbine structure. Vibration reduction fosters other important design goals, such as long fatigue life, high stability and low noise levels. It is one of the main emphasises of this chapter to optimize the system frequencies and investigate their variation with the stiffness and mass distributions of the rotating blades or the supporting tower structures. These frequencies, besides being maximized, must be kept out of the range of the excitation frequencies in order to avoid large induced stresses that can exceed the reserved fatigue strength of the materials and, consequently, cause failure in a short time. Expressed mathematically, two different design criteria are implemented here for optimizing frequencies:

Frequency-placement criterion: Minimize $\sum_i W_{fi}(\omega_i - \omega_i^*)^2$ (4)

Maximum-frequency criterion: Minimize $-\sum_i W_{fi}\omega_i$ (5)

In both criteria, an equality constraint should be imposed on the total structural mass in order not to violate other economic and performance requirements. Equation (4) represents a weighted sum of the squares of the differences between each important frequency ω_i and its desired (target) frequency ω_i^*. Appropriate values of the target frequencies are usually chosen to be within close ranges (called frequency windows) of those corresponding to a reference or baseline design, which are adjusted to be far away from the critical exciting

frequencies. The main idea is to tailor the mass and stiffness distributions in such a way to make the objective function a minimum under the imposed mass constraint. The second alternative for reducing vibration is the direct maximization of the system natural frequencies as expressed by equation (5). Maximization of the natural frequencies can ensure a simultaneous balanced improvement in both of stiffness and mass of the vibrating structure. It is a much better design criterion than minimization of the mass alone or maximization of the stiffness alone. The latter can result in optimum solutions that are strongly dependent on the limits imposed on either the upper values of the allowable deflections or the acceptable values of the total structural mass, which are rather arbitrarily chosen. The proper determination of the weighting factors W_{fi} should be based on the fact that each frequency ought to be maximized from its initial value corresponding to a baseline design having uniform mass and stiffness properties (Negm & Maalawi, 2000).

4.1 Yawing dynamic optimization of combined rotor/tower structure

For wind turbines of horizontal-axis type, the rotation of the nacelle/rotor combination at the top with respect to the tower axis, called yawing motion, is an important degree of freedom in the system dynamics. Such a rigid body motion is produced by the yawing mechanism to direct the rotor towards the wind in order to maximize energy capture. Usually this is accomplished actively with an electrical or hydraulic yaw servo. A wind vane, placed on top of the nacelle, senses the wind direction. The servo is activated when the mean relative wind direction exceeds some predefined limits. Therefore, the wind turbine spends much of its time yawed in order to face the rapidly changing wind direction, so it would seem reasonable to expect that designers should have a sufficient understanding of the turbine response in that condition to take it properly into account. There are frequent yaw system failures world-wide on wind turbines, where some statistical studies indicated that such failures accounts for about 5-10% of breakdowns in any given year the wind plant is in operation. This fact emphasizes the need to improve the design of yaw mechanisms in order to increase the availability of turbines and reduce their maintenance overheads. One of the most cost-effective solutions in designing efficient yaw mechanisms and reducing the produced vibrations is to separate the natural frequencies of the tower/nacelle/rotor structure from the critical exciting yawing frequencies. An optimization model was developed by (Maalawi, 2007) showing the necessary exact dynamical analysis of a practical wind turbine model, shown in Fig. 5, for proper placement of the system frequencies at their target values. The rotor/nacelle combination was considered as a rigid body with mass polar moment of inertia I_N spinning about the vertical axis x at an angular displacement $\psi(t)$ relative to the top of the tower,where t is the time variable. The yawing mechanism was assumed to have a linear torsional spring with a stiffness K_y. The tower is in the state of free torsional vibration about its centroidal axis with an absolute angular displacement denoted by $\varphi(x,t)$. The associated eigenvalue problem is cast in the following:

$$\frac{d}{dx}[GJ(x)\frac{d\Phi}{dx}]+\rho I_p(x)\omega^2\Phi(x)=0 \tag{6}$$

The boundary conditions are:

$$\text{at } x=0 \qquad \Phi(x)=0 \tag{7a}$$

$$\text{at } x=H \qquad \frac{GJ}{\psi_o}\frac{d\Phi}{dx} - K_y = 0\,; \quad \psi_o = \left[\frac{GJ}{\omega^2 I_N}\frac{d\Phi}{dx} - \Phi\right] \tag{7b}$$

where GJ is the torsional rigidity of the tower structure and Φ space–dependent angular displacement.

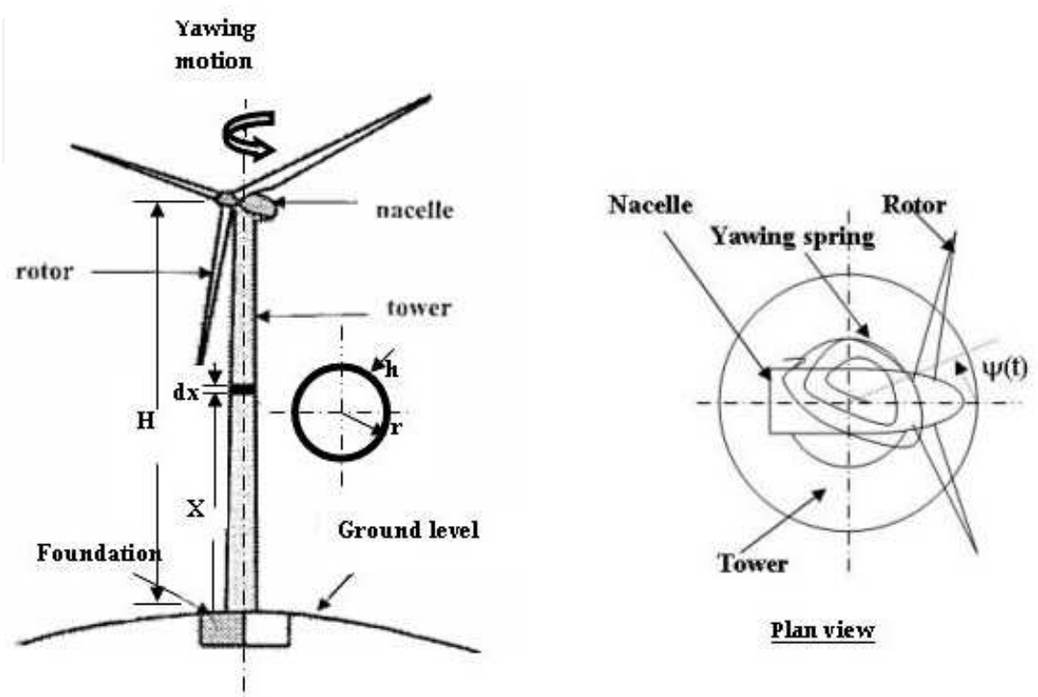

Fig. 5. Horizontal-axis wind turbine in free yawing motion

Considering a tapered, thin-walled tower, the various cross sectional parameters are defined by the following expressions:

$$\text{mean radius} \qquad r = r_o(1 - \beta\hat{x}) \tag{8a}$$

$$\text{wall thickness} \qquad h = h_o(1 - \beta\hat{x}) \tag{8b}$$

$$\text{torsional constant} \quad J = I_p = 2\pi r^3 h \tag{8c}$$

The variables r and h are assumed to have the same linear distribution, and $\hat{x}$ and β are dimensionless quantities defined as:

$$\hat{x} = \frac{x}{H}\,, \quad \beta = (1 - \Delta)\,, \quad \Delta = r_H / r_o \tag{9}$$

where Δ denotes the taper ratio of the wind turbine tower, r_H raduis at height H and r_o at tower base. Quantities with the hat symbol (^) are dimensionless quantities obtained by dividing by the corresponding parameters of a baseline tower design having uniform properties and same structural mass, height and material properties of the optimized tower design (refer to Table 1). Introducing the transformation

$$\hat{x} = \frac{1}{\beta} - \frac{1}{\hat{\omega}} y \quad ; (\beta \neq 0) \tag{10}$$

Equation(6) takes the form:

$$\frac{d^2\Phi}{dy^2} + \frac{4}{y}\frac{d\Phi}{dy} + \Phi = 0 \tag{11}$$

which can be further transformed to the standard form of Bessel's equation by setting $\Phi = (y)^{3/2}\theta$, to get

$$y^2\frac{d^2\theta}{dy^2} + y\frac{d\theta}{dy} + (y^2 - \frac{9}{4})\theta = 0 \tag{12a}$$

which has the solution

$$\theta(y)=C_1J_{3/2}+C_2J_{-3/2} \tag{12b}$$

where C_1 and C_2 are constants of integration and $J_{3/2}$ and $J_{-3/2}$ are Bessel's functions of order $k=\pm 3/2$, given by:

$$J_{3/2}(y) = \sqrt{\frac{2}{\pi y^3}}(\sin y - y\cos y) \tag{13a}$$

$$J_{-3/2}(y)=\sqrt{\frac{2}{\pi y^3}}(\cos y+y\sin y) \tag{13b}$$

Quantity	Notation	Dimensionless expression
Circular frequency	ω	$\hat{\omega} = \omega H\sqrt{\rho/G}$
Spatial coordinate	x	$\hat{x} = x/H$
Tower mean radius	r	$\hat{r} = r/r_b$
Tower wall thickness	h	$\hat{h} = h/h_b$
Tower torsional constant	J	$\hat{J} = J/J_b \ (= \hat{r}^3\hat{h})$
Nacelle/rotor polar moment of inertia	I_N	$\hat{I}_N = I_N/\rho H J_b$
Yawing stiffness coefficient	K_y	$\hat{K}_y = \frac{K_y}{(GJ_b/H)}$
Structural mass	M	$\hat{M} = M/M_b$
Baseline design parameters: M_b=structural mass=$2\pi Hr_bh_b$, J_b=torsional constant of tower cross section (=$2\pi r_b^3h_b$), where r_b=mean radius, h_b=wall thickness; $\hat{\omega}_b$ is the circular frequency=$\pi/2$.		

Table 1. Definition of dimensionless quantities

Finally, the exact analytical solution of the associated eigenvalue problem can be shown to have the form:

$$\Phi(y) = A[\frac{y\cos y - \sin y}{y^3}] + B[\frac{y\sin y + \cos y}{y^3}] \tag{14}$$

where *A* and *B* are constants depend on the imposed boundary conditions:

at $y = \zeta\ (= \hat{\omega}/\beta)$ $\Phi(y)=0$

at $y = \xi\ (= \zeta\Delta)$ $\frac{\hat{\omega}(d\Phi/dy)}{\Psi_o} + (\hat{K}_y/\hat{J}) = 0\,;\quad \Psi_o = [\frac{\hat{J}}{\hat{\omega}\hat{I}_N}\frac{d\Phi}{dy} + \Phi]$ (15)

Applying the boundary conditions, and considering only nontrivial solution of Eq. (14), that is A≠0 and B≠0, it is straightforward to obtain the frequency equation in the following compacted form:

$$\frac{\hat{\omega}^2}{\alpha\hat{\omega} + (\hat{J}/\hat{I}_N)} - (\hat{K}_y/\hat{J}) = 0\,;\quad \alpha = \frac{\xi[\hat{\omega} - (1+\zeta\xi)\tan\hat{\omega}]}{(\xi^2 - 3)(\zeta - \tan\hat{\omega}) + 3\xi(1+\zeta\tan\hat{\omega})} \tag{16}$$

It is to be noticed that in the above equations $\hat{J}$ is the dimensionless torsional constant at the top of tower and is equal to $\hat{r}_o^3\hat{h}_o\Delta^4$ (refer to Eq.8c). The frequency equations for the special cases of the limiting conditions are summarized in Table 2.

Condition	Reduced frequency equation
Locked yawing mechanism ($\hat{K}_y \to \infty$)	$\alpha\hat{\omega} + \hat{J}/\hat{I}_N = 0$
Uniform tower with no taper ($\Delta = 1;\ \beta = 0$)	Apply Eq.(16) with $\alpha = -\tan\hat{\omega}$
Stand-alone tapered tower with no attached masses at the top ($\hat{I}_N = 0$) .	$[(3 - \xi^2) + 3\zeta\xi]\tan\hat{\omega} - [3\hat{\omega} - \zeta\xi^2] = 0$

Table 2. Frequency equation for limiting conditions

Once the exact dimensionless natural frequencies have been determined the associated mode shapes can be obtained analytically from:

$$\Phi(y)=A[(\frac{y\cos y - \sin y}{y^3}) - (\frac{\zeta - \tan\zeta}{1+\zeta\tan\zeta})(\frac{y\sin y + \cos y}{y^3})] \tag{17}$$

Several case studies were investigated and discussed in (Maalawi, 2007). A specific design case for locked yawing mechanism is shown in Fig. 6. It is seen that the objective function is well behaved in the selected design space (Δ, h_o). Actually, the developed chart represent the fundamental frequency function augumented with the imposed mass constraint so that the problem may be treated as if it were an unconstrained optimization problem. Each point inside the chart corresponds to different mass and stiffness distribution along the tower

height, but the total mass is preserved at a constant given value. Now, it is possible to choose the desired frequency, which is far away from the excitation frequencies, and obtain the corresponding optimum variables directly from the chart. It is observed that there is a distinct optimum zone which encompasses the global optimal solution. Results have also indicated that as the rotor/nacelle inertia increases the attained global optimum configuration changes from that one having higher thicknes at tower base with low tapering ration to a configuration with lower thickness and higher tapering ratio. The maximum attainable frequencies for several design cases are summarized in Table 3. The associated optimum values of the chosen design variables, which satisfy the imposed mass equality constraint, are also presented. Fig. 7 shows variation of the optimal fundamental frequency with the yawing stiffness for a practical range of the mass polar moment of inertia of the nacelle/rotor combination in the unlocked condition. As a remarkable observation, the frequency increases for increasing yawing stiffness (K_y) and decreasing the nacelle/rotor inertia (I_N) with a higher rate. The fundamental frequency can be shifted sufficiently from the range which resonates with the excitation yawing frequencies. Other factors that should be considered, as a natural extension of the given formulation, include minimization of the system response to a sudden yaw motion, which can cause severe bending and shearing stresses within the blades and tower structures.

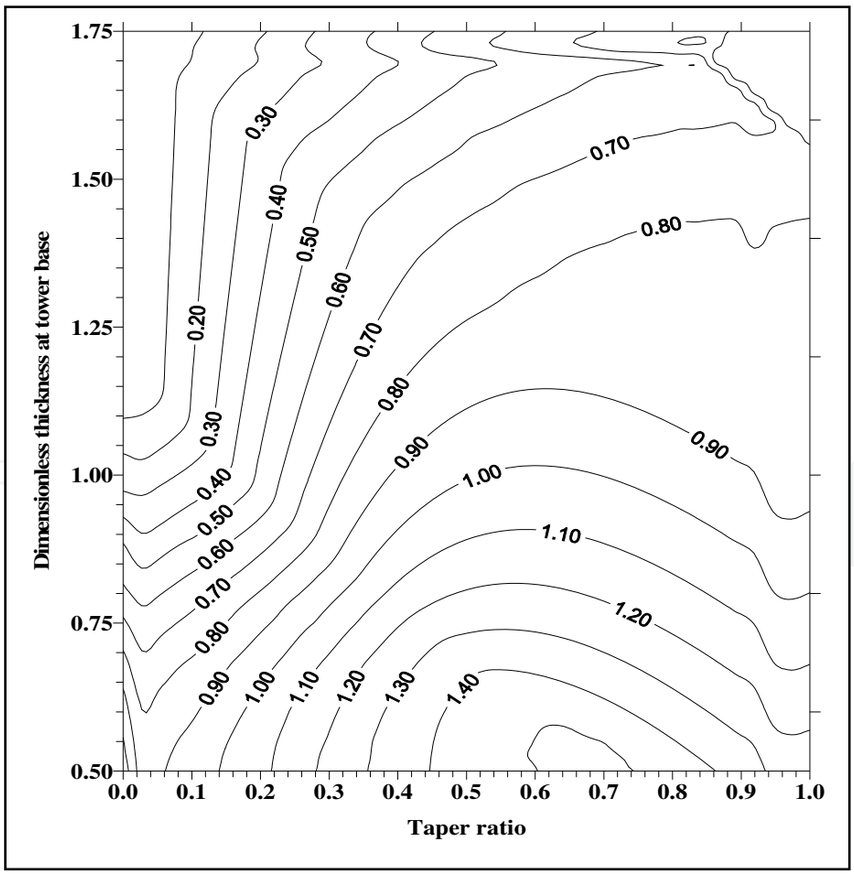

Fig. 6. Frequency chart for a locked yawing mechanism ($\hat{M} = 1$, $\hat{I}_N = 1.0$)

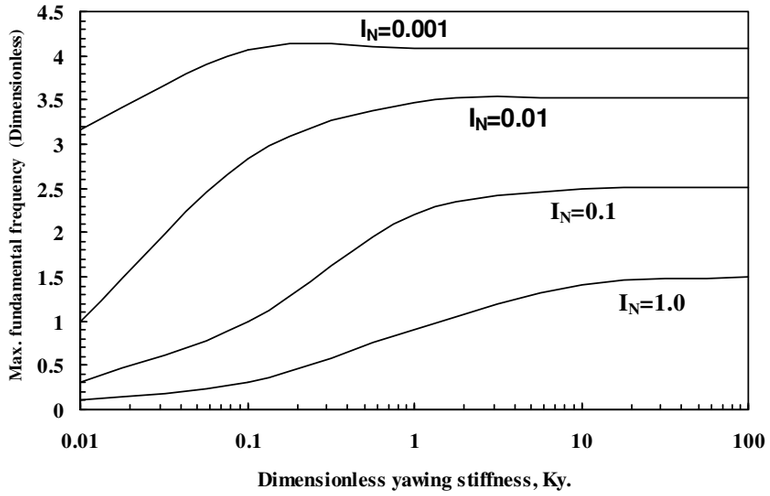

Fig. 7. Variation of the maximum fundamental frequency with yawing stiffness for different inertias of unlocked nacelle/rotor combination, ($\hat{M} = 1.0$)

$\hat{I}_N$ / $\hat{K}_y$	0.001	0.01	0.1	1.0
0.01	3.1625 (0.688,0.6, 2.315)	0.9988 (0.863,0.463,2.489)	0.316 (1.0, 0.4, 2.5)	0.099 (1.0,0.538,1.861)
0.1	4.0663 (0.088,1.10,2.9)	2.833 (0.30,0.875,2.467)	0.9879 (1.0, 0.4, 2.5)	0.3137 (1.0, 0.4, 2.5)
1.0	4.0851 (0.075,1.113,2.495)	3.476 (0.188,0.988,2.485)	2.2105 (0.438,0.738,2.497)	0.9036 (1.0, 0.4, 2.5)
10.0	4.0909 (0.075,1.113,2.495)	3.5191 (0.175,1.0,2.488)	2.4859 (0.375,0.8,2.474)	1.4122 (0.763,0.513,2.497)
(∞) Locked	4.0915 (0.075,1.113,2.495)	3.5241 (0.175,1.0,2.49)	2.515 (0.375,0.8,2.474)	1.50 (0.7,0.55,2.491)

Table 3. Maximum yawing frequency, $\hat{\omega}_{1,max}$ and optimum design variables ($\Delta, \hat{h}_o, \hat{r}_o$)

4.2 Frequency optimization of blades with variable pitch

In strong wind conditions it is necessary to waste part of the excess energy of the wind in order to avoid damaging the wind turbine structure. All wind turbines are therefore designed with some sort of power control. There are different ways of doing this safely on modern wind turbines: pitch, active stall and passive stall controlled wind turbines (Manwell et al., 2009). On a pitch controlled wind turbine the turbine's electronic controller checks the power output of the turbine several times per second. When the power output becomes too high, it sends an order to the blade pitch mechanism which immediately pitches (turns) the rotor blades slightly out of the wind. Conversely, the blades are turned back into the wind whenever the wind drops again. The rotor blades thus have to be able to turn around their longitudinal axis (to pitch) as shown in Fig. 8a. The pitch mechanism is usually operated using hydraulics or electric stepper motors. Fig. 8b shows the optimal

operational conditions of a pitch-controlled 2 MW wind turbine. During normal operation the blades will pitch a fraction of a degree at a time, and the rotor will be turning at the same time. The computer will generally pitch the blades a few degrees every time the wind changes in order to keep the rotor blades at the optimum angle o maximize output power for all wind speeds. (Maalawi & Badr, 2010) formulated an optimization model for avoiding resonance due to blade pitching motion. They considered reduction of vibration either by a direct maximization of the natural frequencies or by separating the natural frequencies of the blade structure from the harmonics of the exciting torque applied from the pitching mechanism at the rotor hub. The derived exact frequency equations for both cases of active and inactive pitching motion are given in the following:

- Baseline design with rectangular planform (Δ=1):

$$\hat{\omega}\tan\hat{\omega} = \hat{K}_S/(\hat{h}_o\hat{C}_o^3) \tag{18a}$$

- Active pitch:

$$\tan\hat{\omega} = \frac{3\hat{\omega}(3+\gamma\delta)}{(\gamma\delta)^2 - 3\gamma^2(1+\Delta^2) + 9(1+\gamma\delta)} \tag{18b}$$

- Inactive pitch:

$$\tan\hat{\omega} = \frac{(1-3\theta)(3\hat{\omega} - \gamma\delta^2) - 3\gamma^2\delta\theta}{3\gamma\delta(1-3\theta) + (3-\delta^2)(1-3\theta+\theta\gamma^2)} \tag{18c}$$

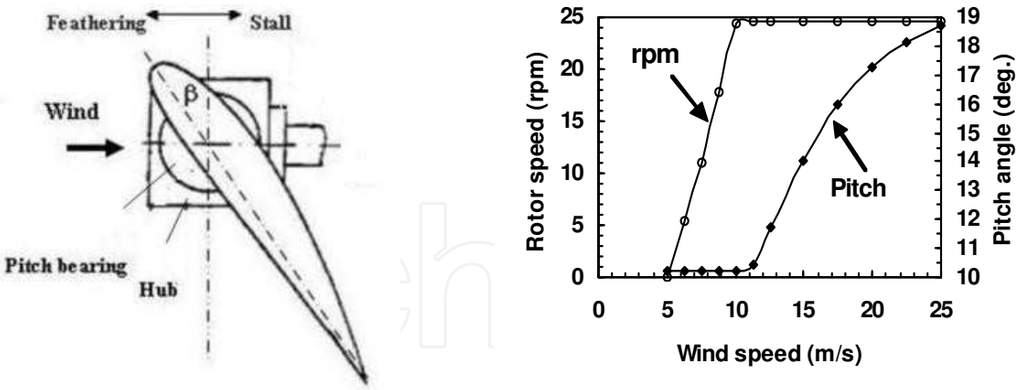

(a) (b)

Fig. 8. Pitch angle (β) and rotational speed (rpm) versus wind speed for a 2 MW turbine

The various parameters in Eq. (18) are defined as follows: h_o= skin thickness at blade root, C_o= airfoil chord at root, K_s=stiffness coefficient at root, Δ=blade tapering ratio, α=(1-Δ), $\gamma = \hat{\omega}/\alpha$, $\delta=\gamma\Delta$ and $\theta = \alpha\hat{h}_o\hat{C}_o^3/\hat{K}_S$. More details can be found in (Maalawi & Badr, 2010), where several case studies were considered. As a demonstration, Fig. 9 depicts the developed frequency chart for the design case of locked pitching mechanism with a flexibile

root having a stiffness coefficient $\hat{K}_S$ =10. The chart can be seen to have a banana-shaped profile bounded by two curved borderlines; the one from above represents a triangular blade geometry (Δ=0) while the lower one represents a rectangular blade geometry (Δ=1). It is not allowed to penetrate these two lines in order not to violate the imposed mass equality constraints. Each point inside the feasible domain in the middle corresponds to different mass and stiffness distributions along the blade span, but the total structural mass is preserved at that value corresponding to a uniform baseline design. The lower and upper empty regions represent, respectively, infeasible blade designs with structural mass less or greater than that of the baseline design. The global optimal design is too close to the design point $\{\hat{C}_o, \hat{h}_o, \Delta\}$={1.202, 2.011, 0.207} with $\hat{\omega}_{1,max}$ =2.6472. If it happened that such global optima violates frequency windows, another value of the frequency can be taken near the optimum point, and an inverse approach is utilized by solving the frequency equation for any one of the unknown design variables instead.

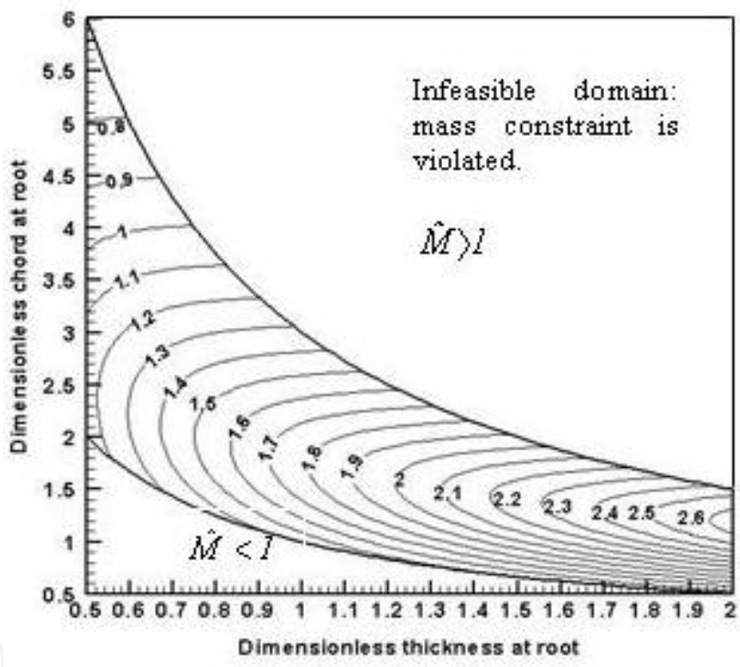

Fig. 9. Augmented pitching frequency-mass contours ($\hat{\omega}_1$) for a blade with flexible root: $\hat{K}_S = 10$ ($\hat{M}$ =1)

4.3 Frequencies of teetered and hingeless blades in flapping motion

Perhaps, the most important degree of freedom in the case of HAWT is the elastic bending deformation perpendicular to the plane of rotation; called flapping motion. Usually, for a typical blade configuration, the chordwise bending (lead-lag) and torsional stiffnesses are much higher than that in the spanwise direction. Therefore, the main focus of this section will be given to flapping dynamics as an important consideration in wind turbine structural design. There are two commonly used types of blade-to-hub connection; namely, teetered and hingless. The teetered type allows rigid body motion of the blades normal to the plane

of rotor disk. It is employed only in one- and two-bladed wind turbines. The teetering rotor has substantial advantages over the hingless rotor with respect to blade shank stresses, fatigue life, and tower loading. The teetering motion of the blades parallel to the power transmission shaft reduces the internal bending stresses in the blades and the vibratory loads transmitted to the supporting tower structure. The only option for the three-bladed rotor is the hingeless type, which is cheaper in construction than the teetered one. However, for wind turbines with power output greater than 6 MW, the decision to whether to select two- or three-bladed rotor is still questionable when considering the overall system design objectives (e.g. cost and fatigue). (Maalawi & Negm, 2002) considered the optimal blade design by maximizing a weighted sum of the flapping frequencies for both teetered and hingeless types. Constraints included avoidance of aeroelastic instabilities, limitations imposed on the total structural mass and capability of starting rotation at the specified cut-in speed. Results showed that the approach used can produce improved designs as compared with known baseline designs. Figs. 10 and 11 show the developed isomerits of the second mode rotating frequency of hingeless and teetered blades, respectively.

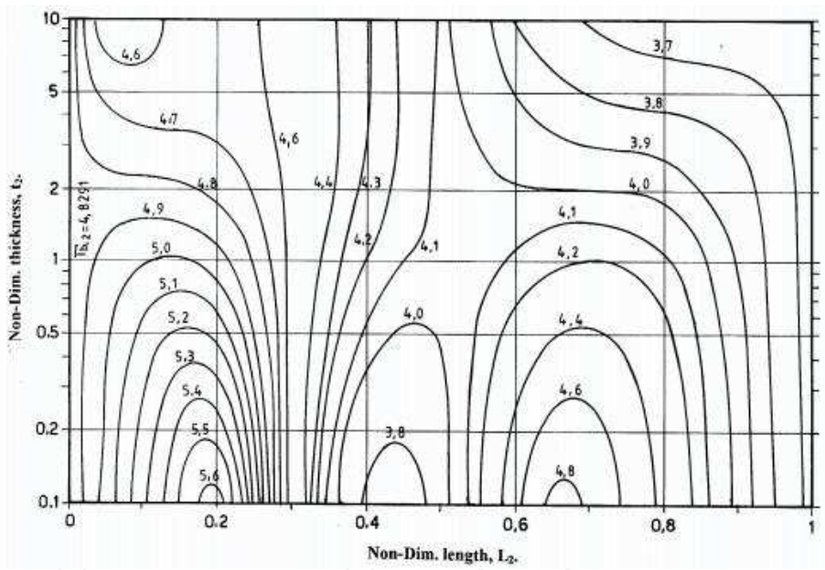

Fig. 10. Second-mode flapping frequency of a hingeless blade

As seen in Fig. 10 the design space contains three distinct frequency branches. The middle one has a local minimum while the one to the left has the global maximum solution. For the teetered type depicted in Fig. 11, there are only two distinguished frequency branches. The one to the left encompasses the global maximum while the one to the right contains a local minimum. The central zone contains a well behaved frequency contours which separate the two branches from each other. It is also observed that, for both types, the global maximum always occurs at the design point which corresponds to the minimum acceptable value of the outboard shear wall thickness.

5. Optimization against buckling

With the development of huge wind turbines, the consideration of inbuckling stability of the supporting tower structure or the rotating blades can be another crucial factor in designing

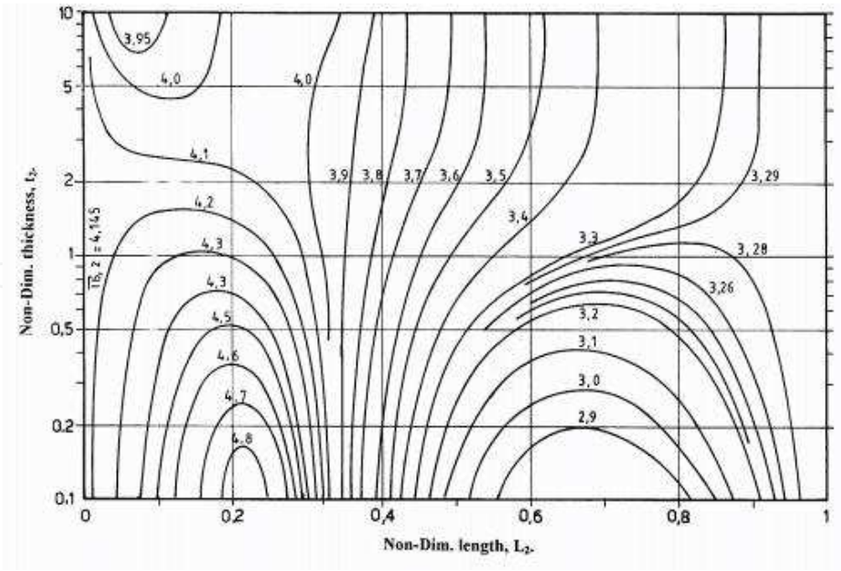

Fig. 11. Second-mode frequency of a teetered blade

efficient wind generators. The tower constructions are usually manufactured as tubular steel sections, which are more economical than solid sections in resisting compressive loads. (Maalawi, 2002) developed an optimization model for maximizing the critical buckling load of elastic columns under equality mass constraint. The given formulation considered columns made of uniform segments with the design variables defined to be the radius of gyration (r_k), wall thickness (t_k) and length (L_k) of each segment. The exact structural analysis ensured the attainment of the absolute maximum critical buckling load for any number of segments, type of cross section and type of boundary conditions. Fig. 12 shows the developed contours of the dimensionless critical buckling load (P_{cr}) for columns having the wall thickness held at its design value in order to avoid the possibility of local buckling of the cylindrical shell structure. The buckling load was found to be very sensitive to variation in the segment length. Investigators who use finite elements have not recognized that the length of each element can be taken as a main variable in addition to the cross-sectional properties.

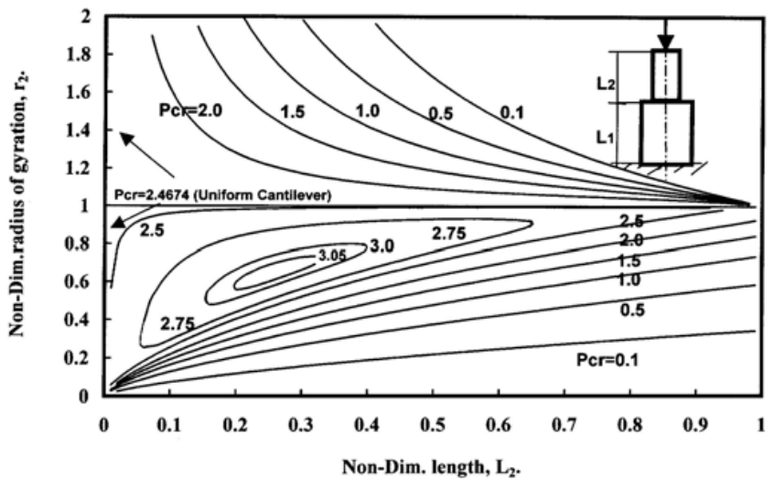

Fig. 12. Optimal buckling design of tubular cantilevers constructed from two segments

Table 4 gives the attained optimal solutions for cantilevers constructed from different number of segments (N_s). About 36% optimization gain was obtained for a cantilever only made of five segments not equally spaced, which represents a truly strongest column design. It is to be noticed that all variables are given in dimensionless form with respect to a known baseline design having uniform properties with the same total length, material properties and cross-sectional type and shape. For example, the critical buckling load P_{cr} shown in Fig. 9 is normalized by the quantity (EI/L^2) of the baseline design, where E=Young's modulus, I=second moment of area and L=total column's length.

Ns	(r_k, L_k), k=1,2,…..,N_s	$P_{cr,max}$	Gain (%)
1	(1,1)	2.467	0
2	(1.117,0.75), (0.65,0.25)	3.072	24.5
3	(1.185,0.507), (0.935,0.333), (0.555, 0.161)	3.248	31.62
4	(1.195,0.495), (0.988, 0.283), (0.687, 0.146), (0.395, 0.077)	3.348	35.70
5	(1.214,0.392), (1.098,0.207), (0.916,0.217), (0.629, 0.109),(0.399, 0.075)	3.368	36.5

Table 4. Optimum tower patterns under mass and local buckling constraints

Another work by (Maalawi, 2009) considered optimization of columns made of composite materials with the design variables taken to be the volume fraction distribution (V) of the constituent materials along the column's length. Results for the optimum columns made of unidirectional composites having the largest possible resistance against buckling are depicted in Fig. 13. It is seen that the increase in the number of segments would, naturally, result in higher values of the critical buckling load. However, care ought to be taken for the corresponding increase in cost of manufacturing procedures.

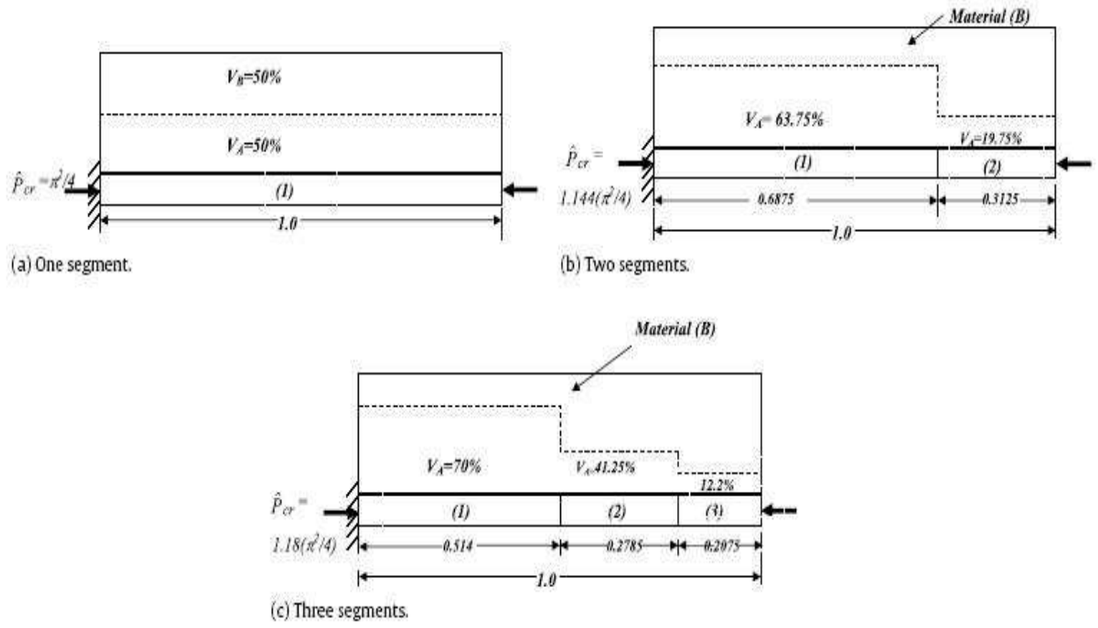

Fig. 13. Strongest columns with axial material grading: Material (A)=E-glass fibers, material (B)=epoxy matrix

6. Material grading for improved aeroelastic stability of composite blades

Wind turbine blades in parked position can experience aeroelstic instability condition for winds coming from all possible directions with speeds ranging from the cut-in up to the survival wind speed. A solution that can be promising to enhance aeroelastic stability of composite blades is the use of the concept of functionally graded materials (FGMs), in which the mechanical and physical properties vary spatially within the structure. FGMs may be defined as advanced composite materials that fabricated to have graded variation of the relative volume fractions of the constituent materials. (Librescu & Maalawi, 2007) introduced the underlying concepts of using material grading in optimizing subsonic wings against torsional instability. They applied an exact mathematical approach allowing the material properties to change in the wing spanwise direction, where both continuous and piecewise structural models were successfully implemented. The enhancement of the torsional stability was measured by maximization of the critical air speed at which divergence occurs with the total structural mass kept at a constant value in order not to violate other performance requirements. Fig. 14 shows a rectangular composite blade model constructed from uniform piecewise panels, where the design variables are defined to be the fiber volume fraction (V_f) and length (L) of each panel. It was shown by many investigators in the field that the use of piecewise models in structural optimization gives excellent results and can be promising for many engineering applications (Negm & Maalawi, 2000).

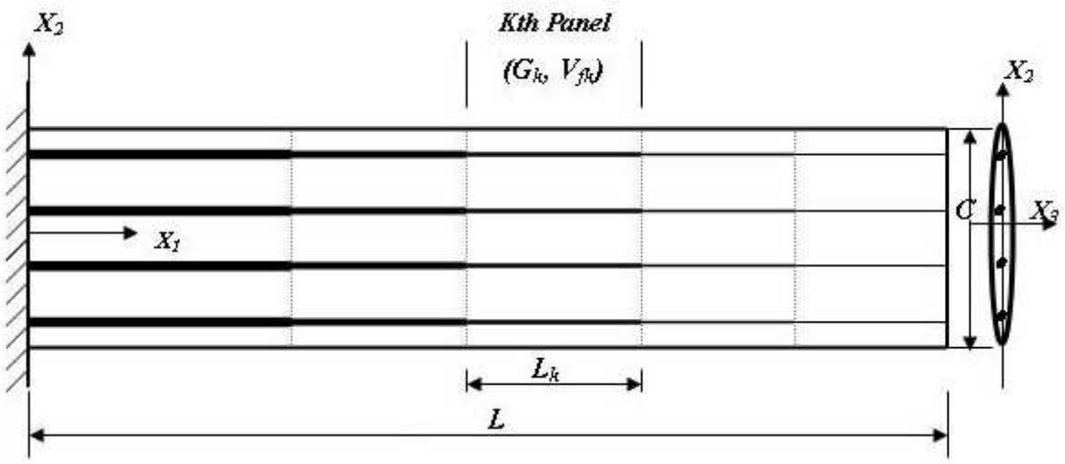

Fig. 14. Composite blade model with material grading in spanwise direction

Fig. 15 shows the isomerits for a blade composed from two panels made of carbon-AS4/epoxy-3501-6 composite. The selected design variables are (V_{f1}, L_1) and (V_{f2}, L_2). However, one of the panel lengths can be eliminated, because of the equality constraint imposed on the blade span. Another variable can also be discarded by applying the mass equality constraint, which further reduces the number of variables to only any two of the whole set of variables. Actually the depicted level curves represent the dimensionless critical air speed augmented with the imposed equality mass constraint. It is seen that the function is well behaved, except in the empty regions of the first and third quadrants, where the equality mass constraint is violated. The final constrained optima was found to be (V_{f1},L_1)= (0.75, 0.5) and (V_{f2},L_2)= (0.25, 0.5), which corresponds to the maximum value of the critical speed of 1.81, representing an optimization gain of about 15% above the reference value $\pi/2$.

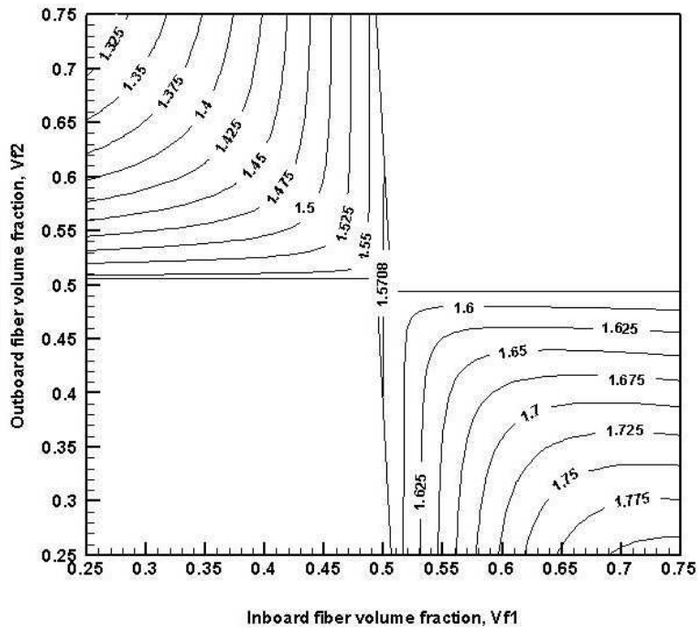

Fig. 15. Isomerits of the normalized divergence speed ($\hat{V}_{div}$) for a two-panel blade model

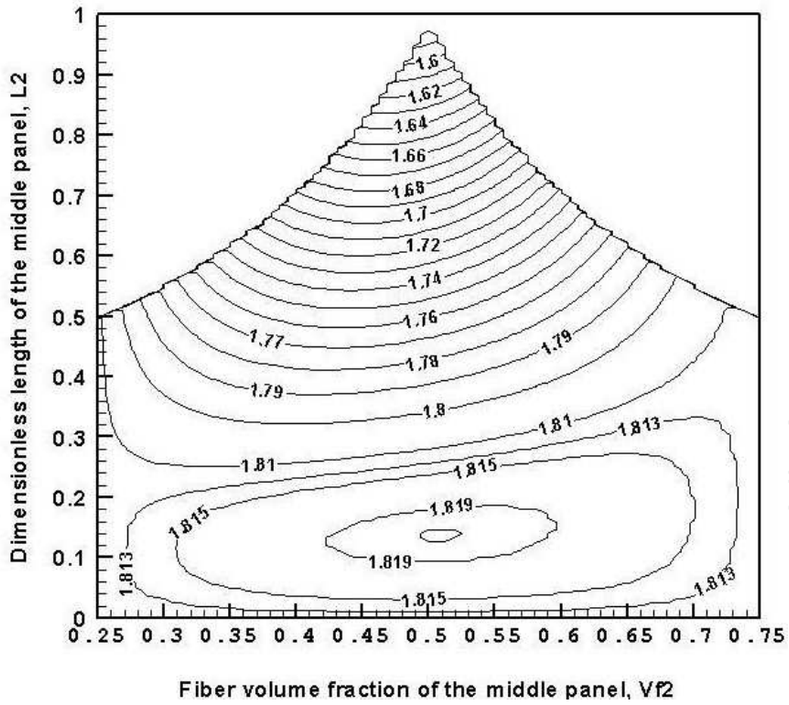

Fig. 16. Isomerits of $\hat{V}_{div}$ in (V_{f2}-L_2) design space for a three-panel model

The functional behavior of the critical air speed $\hat{V}_{div}$ of a three-panel model is shown in Fig. (16), indicating conspicuous design trends for configurations with improved aeroelastic performance. As seen, the developed isomerits has a pyramidal shape with its vertex at the

design point (V_{f2}, L_2)=(0.5, 1.0) having $\hat{V}_{div}=\pi/2$. The feasible domain is bounded from above by the two lines representing cases of two-panel blade, with V_{f1}=0.75 for the line to the left and V_{f3}=0.25 for the right line. The contours near these two lines are asymptotical to them in order not to violate the mass eqaulity constraint. The final global optimal solution, lying in the bottom of the pyramid, was calculated using the MATLAB optimization tioolbox routines as follows: $(V_{fk}, L_k)_{k=1,2,3}$ = (0.75, 0.43125), (0.5, 0.1375), (0.25, 0.43125) with $\hat{V}_{div}$=1.82, which represents an optimization gain of about 16%. Actually, the given exact mathematical approach ensured the attainment of global optimality of the proposed optimization model. A more general case would include material grading in both spanwise and airfoil thickness directions.

7. Conclusion

Wind power is now growing rapidly in the world. Although it currently supplies little of the world's electricity needs, the amount of proposed new wind plants is significant, and could soon make wind the largest source of new power supply generating zero-emissions electricity at an affordable cost. It is the main concern of this chapter to consider system optimization analysis for improving performance and operational efficiency of wind turbines, especially in early stages of product development. Simplified realistic optimization models focusing on both aerodynamic and structural efficiencies of the main structural components, namely; the rotating blades and the supporting tower structures are presented and discussed. Design variables encompass blade and tower geometry as well as cross-sectional parameters. Different strategies have been addressed, including power output maximization, blade optimization in flapping and pitching motion and yawing dynamic optimization of combined rotor/tower structure. Optimization of the supporting tower structure against buckling as well as the use of the concept of material grading for enhancing the aeroelastic stability of composite blades have been also addressed. It has been shown that normalization of all terms results in a naturally scaled objective functions, constraints and design variables, which is recommended when applying different optimization techniques. Several design charts that are useful for direct determination of the optimal values of the design variables are given. The various approaches that are commonly utilized in design optimization are also presented with a brief discussion of some computer packages classified by their specific applications. Another promising area of future research is the development of topology optimization methods to simultaneously design smart wind turbine structures. Actually, the most economic design that will perform its intended function with adequate safety and durability requires much more than the procedures that have been described in this chapter. Further optimization studies must depend on a more accurate analysis of constructional cost. This combined with probability studies of load applications and materials variations, should contribute to further efficiency achievement. Finally, much improved and economical designs for wind turbines may be obtained by considering multi-disciplinary design optimization, which allows designers to incorporate all relevant design objectives simultaneously.

8. References

Burger, C. & Hartfield, R. (2006). Wind turbine airfoil performance optimization using the vortex lattice method and genetic algorithm. 4th AIAA Energy Conversion Engineering Conference, June 2006, AIAA 2006-4051, 26-29.

Cobb, R., Canfield, R. and Liebst, B. (1996). Finite element model tuning using automated structural optimization system software. *AIAA Journal*, Vol. 34, No.2, 392-399, ISSN: 0001-1452.

Kusiak A., Zheng H. and Song Zhe (2009). Power optimization of wind turbines with data mining and evolutionary computation. *Renewable energy*, Vol.35, 695-702.

Librescu, L. & Maalawi, K. (2007). Material grading for improved aeroelastic stability in composite wings. *Journal of Mechanics of Materials and Structures,* Vol.2, No.7, 1381-1394.

Maalawi, K. & Badawy, M. (2001). A direct method for evaluating performance of horizontal axis wind turbines. *Renewable and Sustainable Energy Reviews,* Vol.5, No.2, 175-190.

Maalawi, K. & Negm, H. (2002). Optimal frequency design of wind turbine blades. *Journal of Wind Engineering and Industrial Aerodynamics,* Vol.90, No.8, 961-986.

Maalawi, K. (2002). Buckling optimization of flexible columns. *International Journal of Solids and Structures,* Vol.39, 5865-5876.

Maalawi, K. & Badr, M. (2003). A practical approach for selecting optimum wind rotors. *International Journal of Renewable Energy,* Vol.28, No.5, 803-822.

Maalawi, K. (2007). A model for yawing dynamic optimization of a wind turbine structure. *International Journal of Mechanical Sciences,* Vol.49, No.10, 1130-1138.

Maalawi, K. (2009). Optimization of elastic columns using axial grading concept. *Engineering Structures,* Vol.31, No.12, 2922-2929.

Maalawi, K. & Badr, M. (2010). Frequency optimization of a wind turbine blade in pitching motion. *Proceedings of the Institution of Mechanical Engineers, Part A: Journal of Power and Energy,* Vol.224 (A4), No.2, 545-554, Professional Engineering Publisher, ISSN: 0957-6509JPE907.

Manwell, J.; McGowan, J. & Rogers, A. (2009). *Wind Energy Explained: Theory, Design & Application,* 2nd edition, Wiley, ISBN-13: 978-0470015001, United Kingdom.

Negm, H. & Maalawi K. (2000). Structural design optimization of wind turbine towers. *Computers and Structures,* Vol.74, No.6, 649-666.

Overgaard, L.C.T. & Lund E. (2005). Structural design sensitivity analysis and optimization of Vestas V52 wind turbine blade, *Proceedings of the 6th World Congress on Structural and Multidisciplinary Optimization*, CD-ROM, 10 pages, ISBN: 85-285-0070-5, Rio de Janeiro, 30 May-03 June 2005, Brazil.

Rao, S. (2009). *Engineering Optimization: Theory and Practice,* 4th edition, John Wiley & Sons, ISBN: 978-0470183526, New York.

Spera, D. (2009). *Wind Turbine Technology: Fundamental Concept in Wind Turbine Engineering,* 2nd edition, ASME Press, ISBN-13: 978-0791802601, New York.

Venkataraman, P. (2009). *Applied Optimization with MATLAB Programming,* 2nd edition, John Wiley & Sons, ISBN: 978-0470084885, New York.

Wei Tong (2010). *Wind Power Generation and Wind Turbine Design*, WIT Press, ISBN: 978-1845642051, United Kingdom.

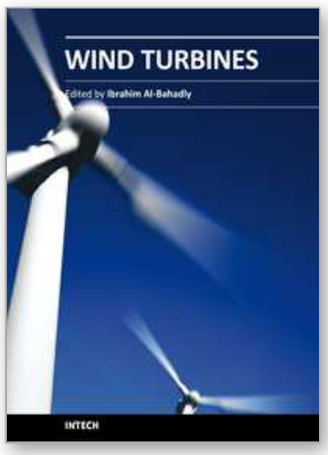

Wind Turbines

Edited by Dr. Ibrahim Al-Bahadly

ISBN 978-953-307-221-0
Hard cover, 652 pages
Publisher InTech
Published online 04, April, 2011
Published in print edition April, 2011

The area of wind energy is a rapidly evolving field and an intensive research and development has taken place in the last few years. Therefore, this book aims to provide an up-to-date comprehensive overview of the current status in the field to the research community. The research works presented in this book are divided into three main groups. The first group deals with the different types and design of the wind mills aiming for efficient, reliable and cost effective solutions. The second group deals with works tackling the use of different types of generators for wind energy. The third group is focusing on improvement in the area of control. Each chapter of the book offers detailed information on the related area of its research with the main objectives of the works carried out as well as providing a comprehensive list of references which should provide a rich platform of research to the field.

INTECH
open science | open minds

InTech Europe
University Campus STeP Ri
Slavka Krautzeka 83/A
51000 Rijeka, Croatia
Phone: +385 (51) 770 447
Fax: +385 (51) 686 166
www.intechopen.com

InTech China
Unit 405, Office Block, Hotel Equatorial Shanghai
No.65, Yan An Road (West), Shanghai, 200040, China
中国上海市延安西路65号上海国际贵都大饭店办公楼405单元
Phone: +86-21-62489820
Fax: +86-21-62489821

IntechOpen